Article

Cell Reports

Identification and Targeting of Long-Term Tumor-Propagating Cells in Small Cell Lung Cancer

Graphical Abstract

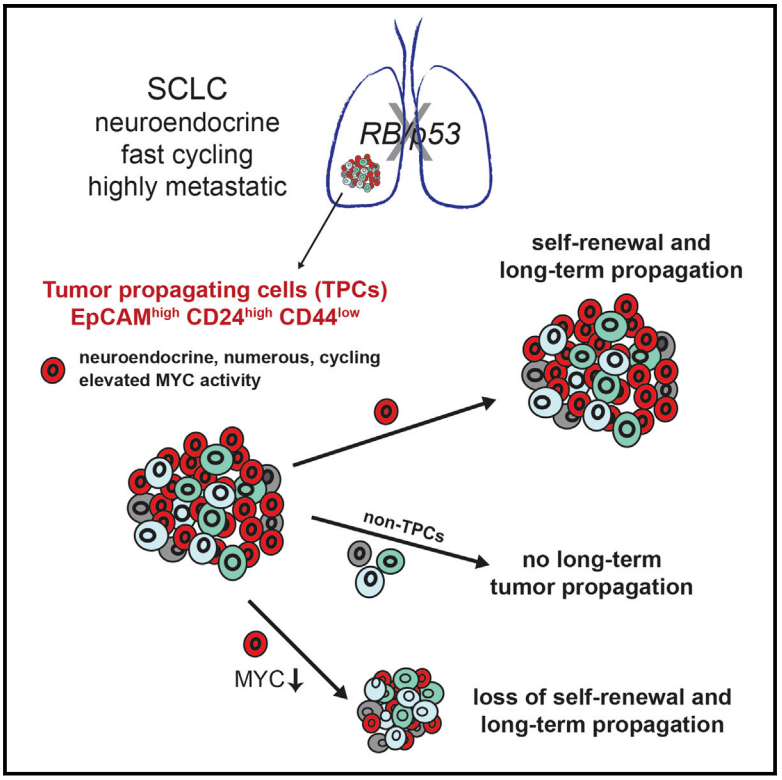

Authors

Nadine S. Jahchan, Jing Shan Lim, Becky Bola, ..., Martin Peifer, Caroline Dive, Julien Sage

Correspondence

julsage@stanford.edu

In Brief

Jahchan et al. use a genetically engineered mouse model of small cell lung cancer (SCLC) to functionally characterize cancer stem cells (tumor-propagating cells, TPCs). SCLC TPCs are numerous in tumors, cycle quickly, are chemosensitive, and depend on elevated MYC activity for their ability to propagate tumors.

Highlights

- $CD24^{High}$ $CD44^{Low}$ $EpCAM^{High}$ mark tumor-propagating cells (TPCs) in mouse SCLC
- SCLC TPCs generate non-TPCs and are proliferative and abundant but not chemoresistant
- Elevated MYC activity is required for the maintenance of TPCs in SCLC tumors
- A low dose of the transcriptional inhibitor JQ1 inhibits long-term SCLC growth

Accession Number

GSE72406

Jahchan et al., 2016, Cell Reports *16*, 644–656
July 19, 2016
http://dx.doi.org/10.1016/j.celrep.2016.06.021

OPEN ACCESS
CellPress

Cell Reports
Article

Identification and Targeting of Long-Term Tumor-Propagating Cells in Small Cell Lung Cancer

Nadine S. Jahchan,[1,2] Jing Shan Lim,[1,2] Becky Bola,[3] Karen Morris,[3] Garrett Seitz,[1,2] Kim Q. Tran,[1,2] Lei Xu,[1,2] Francesca Trapani,[3] Christopher J. Morrow,[3] Sandra Cristea,[1,2] Garry L. Coles,[1,2] Dian Yang,[1,2] Dedeepya Vaka,[1,2] Michael S. Kareta,[1,2] Julie George,[5] Pawel K. Mazur,[1,2] Thuyen Nguyen,[1,2] Wade C. Anderson,[6] Scott J. Dylla,[6] Fiona Blackhall,[4] Martin Peifer,[5] Caroline Dive,[3] and Julien Sage[1,2,*]

[1]Department of Pediatrics
[2]Department of Genetics
Stanford University School of Medicine, Stanford, CA 94305, USA
[3]Clinical and Experimental Pharmacology Group, Cancer Research UK Manchester Institute
[4]Institute of Cancer Sciences
University of Manchester and Manchester Cancer Research Centre, Wilmslow Road, Manchester M20 4BX, UK
[5]Medical Faculty, Department of Translational Genomics, Center of Integrated Oncology Cologne–Bonn and Center for Molecular Medicine Cologne (CMMC), University of Cologne, 50931 Cologne, Germany
[6]Stemcentrx Inc., South San Francisco, CA 94080, USA
*Correspondence: julsage@stanford.edu
http://dx.doi.org/10.1016/j.celrep.2016.06.021

SUMMARY

Small cell lung cancer (SCLC) is a neuroendocrine lung cancer characterized by fast growth, early dissemination, and rapid resistance to chemotherapy. We identified a population of long-term tumor-propagating cells (TPCs) in a mouse model of SCLC. This population, marked by high levels of EpCAM and CD24, is also prevalent in human primary SCLC tumors. Murine SCLC TPCs are numerous and highly proliferative but not intrinsically chemoresistant, indicating that not all clinical features of SCLC are linked to TPCs. SCLC TPCs possess a distinct transcriptional profile compared to non-TPCs, including elevated MYC activity. Genetic and pharmacological inhibition of MYC in SCLC cells to non-TPC levels inhibits long-term propagation but not short-term growth. These studies identify a highly tumorigenic population of SCLC cells in mouse models, cell lines, and patient tumors and a means to target them in this most fatal form of lung cancer.

INTRODUCTION

Small cell lung cancer (SCLC), which represents ~15% of lung cancers, is characterized by small cells with neuroendocrine features (Wistuba and Gazdar, 2006). Close to 200,000 people die from SCLC every year worldwide, and the 5-year survival rate is a dismal 5%–10%. SCLC disseminates early and is usually detected late when patients present with extensive metastases. Patients often respond well initially to chemotherapy (usually a combination of etoposide and a platinum-based agent), but they almost invariably relapse with disease that is resistant to their primary therapy and other agents. Despite numerous clinical trials, no new treatment has been approved in two decades and SCLC remains the most lethal form of lung cancer (Pietanza et al., 2015).

The cancer stem cell model assumes a hierarchical organization in which a subset of tumor cells is responsible for sustaining tumorigenesis and establishing the cellular heterogeneity of a primary tumor (Beck and Blanpain, 2013; Clarke et al., 2006; Magee et al., 2012; Visvader and Lindeman, 2012). Not all tumors may be organized in such a hierarchical manner (Meacham and Morrison, 2013; Quintana et al., 2010). The aggressive and highly metastatic nature of SCLC tumors suggests that SCLC tumors may harbor highly tumorigenic cells. However, the study of SCLC is challenging in patients because of the inherent complex genetic and environmental diversity of these patients. SCLC patients rarely undergo surgery, and primary human material is scarce. Moreover, the establishment of SCLC cell lines and patient-derived xenografts can select for the growth of specific populations of tumor cells (Daniel et al., 2009; Leong et al., 2014), which may bias the analysis of cancer cell subpopulations. In contrast, relevant mouse models allow for the analysis of large number of independent primary tumors. The first mouse model for SCLC was developed based on the observation that human SCLCs are mutant for both the p53 and the RB tumor suppressors (Meuwissen et al., 2003). The additional deletion of the *p130* gene (also known as *Rbl2*) enhances SCLC development (Schaffer et al., 2010). Tumors that are triple knockout (TKO) for *Rb* (also known as *Rb1*), *p130*, and *p53* (also known as *Tp53*) have histopathological features of human SCLC, including an initial relative chemosensitivity followed by the acquisition of chemoresistance (Gazdar et al., 2015; Jahchan et al., 2013; Park et al., 2011).

Here we use mouse models and human SCLC cells to investigate tumor heterogeneity in SCLC. Because cancer stem cells may not possess the exact and full repertoire of normal tissue stem cell properties, we instead use the term tumor-propagating cells (TPCs). We define TPCs as cells that are highly tumorigenic

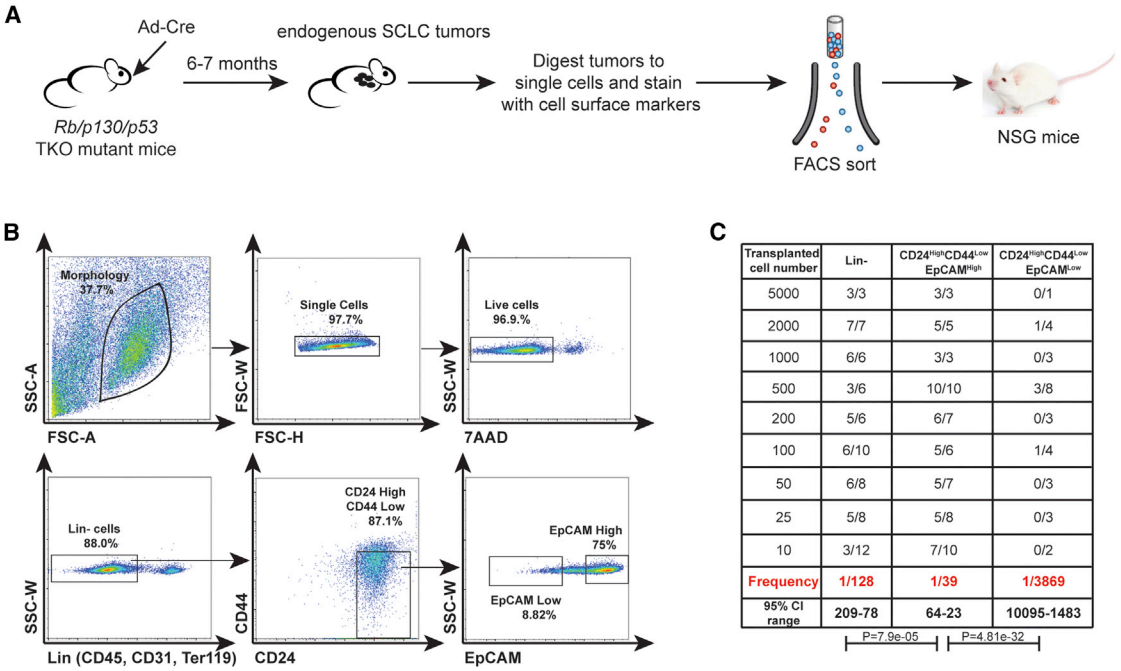

Transplanted cell number	Lin-	$CD24^{High}CD44^{Low}$ $EpCAM^{High}$	$CD24^{High}CD44^{Low}$ $EpCAM^{Low}$
5000	3/3	3/3	0/1
2000	7/7	5/5	1/4
1000	6/6	3/3	0/3
500	3/6	10/10	3/8
200	5/6	6/7	0/3
100	6/10	5/6	1/4
50	6/8	5/7	0/3
25	5/8	5/8	0/3
10	3/12	7/10	0/2
Frequency	**1/128**	**1/39**	**1/3869**
95% CI range	**209-78**	**64-23**	**10095-1483**

Figure 1. Mouse SCLC Tumors Contain a High Fraction of Tumor-Propagating Cells in Transplantation Assays

(A) Workflow to identify TPCs in a pre-clinical mouse model of SCLC (TKO, *Rb/p53/p130* mutant).

(B) Representative flow cytometry analysis of TKO SCLC cells with markers of cell death (7AAD), lineage (CD45, CD31, and Ter119), CD24, CD44, and EpCAM ($n > 20$).

(C) ELDA of lineage-negative (Lin^-, bulk tumor cells), $CD24^{High}$ $CD44^{Low}$ $EpCAM^{High/Low}$ cells sorted from TKO tumors and injected subcutaneously in NSG mice. See also Figure S1.

in transplantation assays and that can self-renew and differentiate into the bulk tumor population. We found that SCLC TPCs are highly abundant and are proliferative but not inherently chemoresistant in a mouse model. We also identified similar populations marked by high levels of the cell surface markers EpCAM and CD24 and low levels of CD44 in primary human explant models. Finally, we identified elevated MYC activity, in particular L-MYC, as a key determinant of the ability of SCLC TPCs to maintain the long-term growth of SCLC tumors.

RESULTS

SCLC Tumors Contain a High Fraction of TPCs

To investigate the presence of TPCs in primary *Rb/p130/p53* TKO tumors, we injected serial dilutions of tumor cell suspensions subcutaneously into Nod.Cg-Prkdc^{scid}IL2rg^{tm1Wjl}/SzJ (NSG) mice (Figures 1A and 1B). In these assays, the calculated frequency of tumor initiation was ~1/128 (Figure 1C). This number is more than ten times higher than the number observed with mouse models of lung adenocarcinoma (Zheng et al., 2013) and is similar to that of highly aggressive breast cancer models (Vaillant et al., 2008), suggesting that TPCs may be abundant in murine SCLC tumors.

We next examined cell surface markers previously associated with TPCs in a few SCLC cell lines or in other solid tumor types, including CD133 (Jiang et al., 2009; Sarvi et al., 2014), CD90 (Salcido et al., 2010; Wang et al., 2013), c-KIT (Micke et al., 2003; Rygaard et al., 1993), and hepatocyte growth factor receptor (HGFR) (Rygaard et al., 1993). Transplantation trials with 500–5,000 mouse tumor cells sorted for each of these markers independently showed no trend in enrichment (or loss) of tumorigenic potential (data not shown). In contrast, high levels of CD24 enriched for TPCs, and the transplantation ability of $CD24^{High}$ cells was further increased by selecting for $CD44^{Low}$ and $EpCAM^{High}$ cells (Figures 1B, 1C, S1A, and S1B). Using a tumor-specific GFP reporter, we found that both TPC and non-TPC populations identified by these three markers are tumor cells (Figures S1C and S1D). These populations were also found in individually dissected tumors (Figure S1E) and in an *Rb/p53* mutant primary tumor (Figure S1F). Overall, $CD24^{High}$ $CD44^{Low}$ $EpCAM^{High}$ SCLC cells represent ~50% of live tumor cells (Figure S1G). Thus, TKO tumors harbor a high number of SCLC cells with the ability to transplant tumors, and the combination of $CD24^{High}$, $CD44^{Low}$, and $EpCAM^{High}$ identifies cells that transplant 100 times more efficiently than other SCLC cell populations. We found that SCLC cells seed tumors in the liver but not the lungs following intravenous injection and do not reliably form lung tumors following intratracheal instillation, preventing us from investigating TPCs in an orthotopic model (data not shown).

SCLC patients rarely undergo surgery, and we were not able to perform transplantation assays with fresh human specimens. Nevertheless, *EPCAM* and *CD24* mRNA levels are high and *CD44* expression is low in human SCLC cell lines and primary bulk tumors (Figure S2A). Circulating tumor cells (CTCs) from

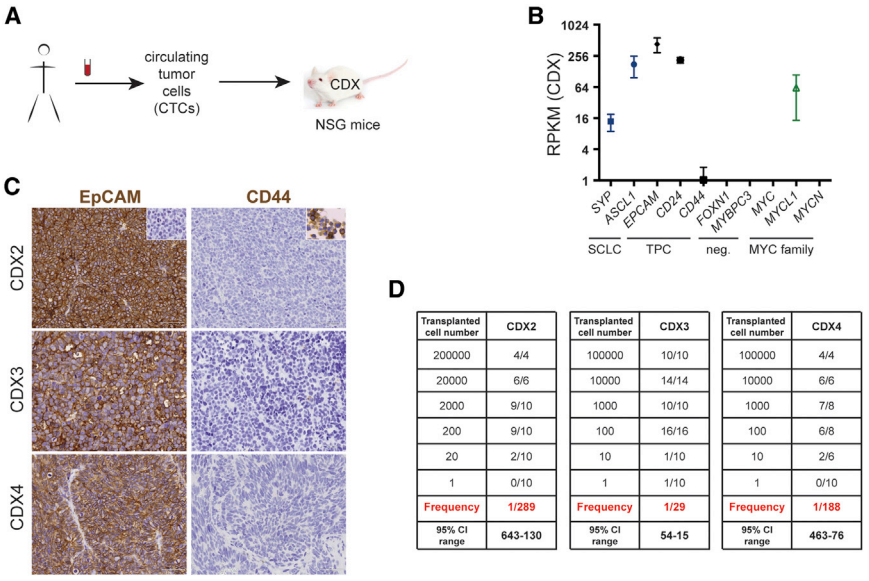

Transplanted cell number	CDX2
200000	4/4
20000	6/6
2000	9/10
200	9/10
20	2/10
1	0/10
Frequency	1/289
95% CI range	643-130

Transplanted cell number	CDX3
100000	10/10
10000	14/14
1000	10/10
100	16/16
10	1/10
1	1/10
Frequency	1/29
95% CI range	54-15

Transplanted cell number	CDX4
100000	4/4
10000	6/6
1000	7/8
100	6/8
10	2/6
1	0/10
Frequency	1/188
95% CI range	463-76

Figure 2. Xenografts Derived from Human SCLC CTCs Harbor a High Frequency of TPCs and High Numbers of CD24^{High} CD44^{Low} EpCAM^{High} Cells

(A) Workflow to generate xenografts (CDXs) derived from human SCLC CTCs.

(B) Expression (reads per kilobase of transcript per million mapped reads [RPKM], from RNA sequencing) of two genes expressed at high levels in SCLC (*ASCL1* and *SYP*) compared to the TPC markers *EPCAM*, *CD24*, and *CD44* (n = 3 CDXs). Negative controls: *FOXN1*, thymic and skin epithelium; *MYBPC3*, heart. Levels of the three *MYC* genes are also shown.

(C) Immunostaining for EpCAM and CD44 (brown signal) on CDX models. Lymphoma SUDHL8 cells were used as a negative control for EpCAM (left inset), and H196 lung cancer cells were used as a positive control for CD44 (right inset). Counterstain was hematoxylin. Scale bars, 100 μm.

(D) ELDA of cells from the CDX2, CDX3, and CDX4 models. The data for CDX2 and CDX4 are not statistically different, but the lower frequency for CDX3 is (p values of 1.12×10^{-07} for the CDX2 comparison and 3.51×10^{-05} for CDX4).

See also Figure S2.

SCLC patients form CDX (CTC-derived explant) tumors with a take rate of ~50% under the skin of NSG mice (Figure 2A) (Hodgkinson et al., 2014; Krebs et al., 2014). Although human SCLC CTCs are not enriched for EpCAM expression before assaying their transplantation ability and EpCAM^{-} CTCs can be found in the blood of SCLC patients (Chudziak et al., 2016), CDX tumors express high mRNA levels of *CD24* and *EpCAM* and low levels of *CD44* (Figure 2B). Fluorescence-activated cell sorting (FACS) analysis on three CDX models showed that an average of 41% of human SCLC cells was CD24^{High} CD44^{Low} EpCAM^{High} (42%, 27%, and 55% for CDX2, CDX3, and CDX4, respectively) (Figure S2C). These observations were confirmed by immunostaining for EpCAM and CD44 on tumor sections (Figure 2C). The frequency of TPCs using single cells dissociated from CDX models was similar to that seen with mouse TKO TPCs (compare Figure 2D to Figure 1C). Cells in patient-derived xenografts (PDXs) (e.g., PDX model LU95) were nearly exclusively CD24^{High} CD44^{Low} EpCAM^{High}, and EpCAM^{+} cells were able to confer tumorigenicity (Figure S2D) (Saunders et al., 2015). High levels of EpCAM expression (but not CD24; data not shown) in early-stage tumors (George et al., 2015) correlated with decreased survival in SCLC patients (Figure S2E), suggesting that a high level of EpCAM is associated with more aggressive tumors.

CD24^{High} CD44^{Low} EpCAM^{High} Mouse SCLC Cells Give Rise to TPCs and Non-TPCs and Can Be Serially Transplanted

We next tested the long-term propagation ability of CD24^{High} CD44^{Low} EpCAM^{High} SCLC cells, focusing on TKO tumors because of the availability of numerous primary tumors (Figure 3A). TKO CD24^{High} CD44^{Low} EpCAM^{High} SCLC cells could generate new tumors at a similar frequency each time they were passaged (Figures 3A and S3A). The passaged tumors retained histopathological features of SCLC tumors, including expression of the neuroendocrine markers ubiquitin-C-terminal hydrolase 1 (Uchl1, also known as PGP9.5) and Ascl1 (Figures 3B and S3B). In addition, tumors initiated by CD24^{High} CD44^{Low} EpCAM^{High} cells gave rise to all subpopulations of cells found in primary tumors (Figure 3C). CD24^{High} CD44^{Low} EpCAM^{High} cells were not quiescent and had similar proliferative rates compared to CD24^{High} CD44^{Low} EpCAM^{Low} cells or to all non-TPCs populations combined (Figures 3D, 3E, and S3C). Thus, actively cycling CD24^{High} CD44^{Low} EpCAM^{High} SCLC cells self-renew and are enriched for the ability to propagate all tumor populations in this mouse model.

CD24^{High} CD44^{Low} EpCAM^{High} TPCs Are Not Inherently Chemoresistant

Cancer stem cells have been associated with chemoresistance and tumor relapse (Shafee et al., 2008; Visvader and Lindeman, 2012; Zheng et al., 2013). To investigate how TPCs responded to chemotherapy compared to non-TPCs, TKO mice carrying an inducible luciferase reporter allele (*Rosa26$^{lox\text{-}Stop\text{-}lox\text{-}Luciferase}$*) were monitored for tumor development in response to chemotherapy. At the end of each experiment, the relative frequency of TPCs was assessed by flow cytometry. Acute treatment with high doses of cisplatin and etoposide (Figure 4A) led to a significant induction of apoptosis in tumors, as monitored by cleaved caspase-3 (CC3) immunostaining (Figures 4B and S4A), but there was no difference in the frequency of cells with TPC markers (CD24^{High} CD44^{Low} EpCAM^{High}) versus non-TPCs (CD24^{High} CD44^{Low} EpCAM^{Low}, CD24^{Low}, and CD24^{High} CD44^{High}) in this assay (Figures 4C and S4B). Analysis of TPCs and non-TPCs following 6 days of recovery after 3 days of acute treatment in a similar setting showed no differences in the relative percentages for these two populations; in addition, we observed no differences in the proliferative rate of TPCs from

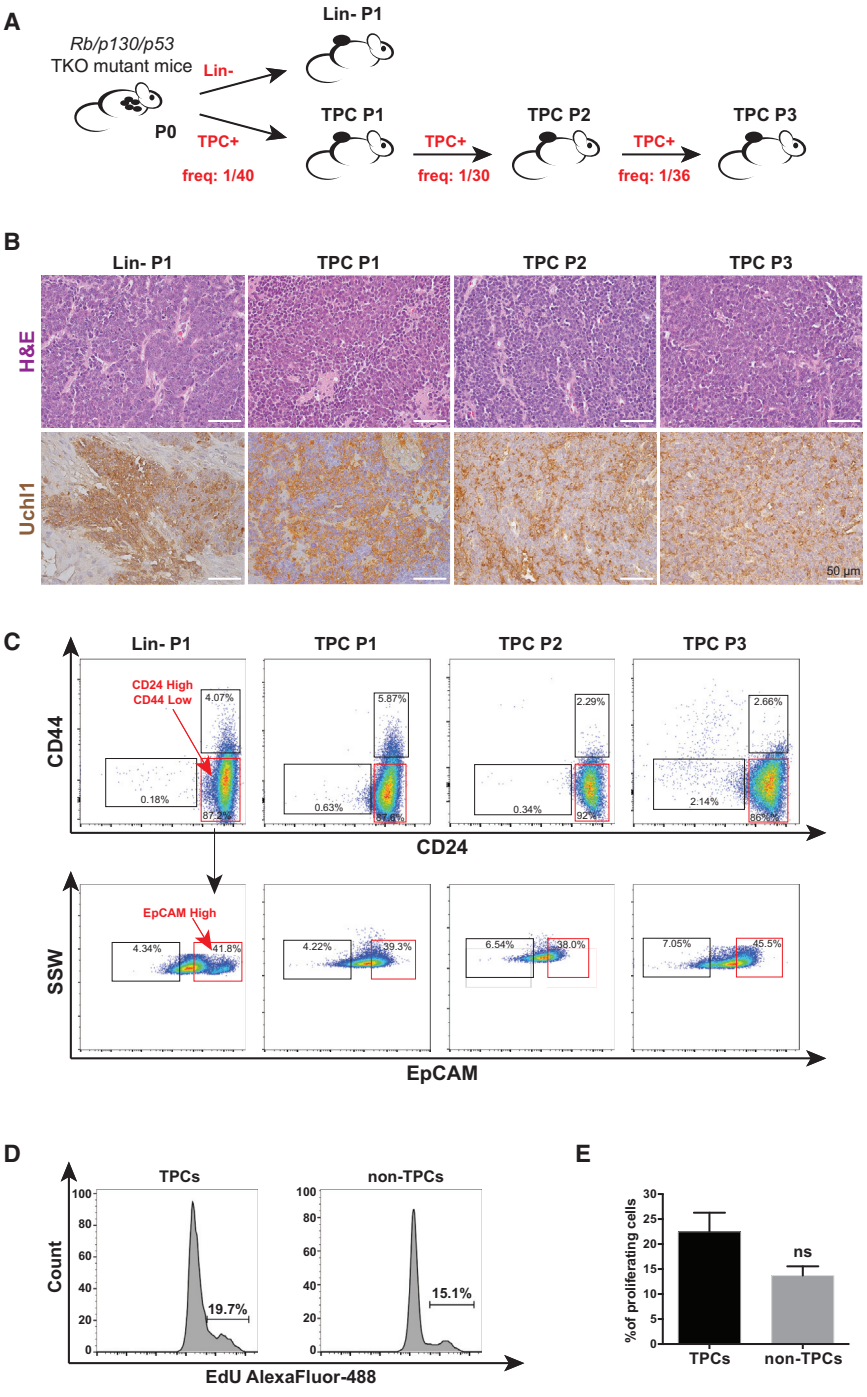

Figure 3. Serial Transplantation Reveals a Stable TPC Phenotype in the Murine CD24^{High} CD44^{Low} EpCAM^{High} SCLC Cell Population

(A) Serial transplantation assays (passages P1, P2, and P3) of sorted lineage-negative cells (Lin$^-$: CD45$^-$, CD31$^-$, and Ter119$^-$) and TPCs (CD24^{High} CD44^{Low} EpCAM^{High}) from TKO tumors (P0). The estimated frequency of tumor formation is shown in red. Tumors from two TKO mice were passaged to P3, and analysis was done on a minimum of two allografts per passage for each.

(B) Representative sections from the Lin$^-$ P1, TPC P1, TPC P2, and TPC P3 allografts counterstained with H&E or immunostained for the neuroendocrine marker Uchl1. Scale bars, 50 μm.

(C) Representative FACS plots of TPCs (red boxes) and non-TPCs (black boxes) from Lin$^-$ P1, TPC P1, TPC P2, and TPC P3 allografts (n > 2).

(D) Representative FACS histograms of TPCs and non-TPCs (CD24^{High} CD44^{Low} EpCAM^{Low}) tumor subpopulations labeled with the DNA replication marker EdU.

(E) Bar chart showing the frequency of EdU$^+$ cycling cells in TPCs and non-TPCs (CD24^{High} CD44^{Low} EpCAM^{Low}) tumor subpopulations from three different *Rb/p53/p130* mutant mice. CD24^{High} CD44^{High} and CD24^{Low} populations also showed non-significant differences in EdU incorporation (data not shown). NS, not significant; error bars represent mean ± SEM (n = 3 mice); p values are from a paired t test (p = 0.1151).

See also Figure S3 for information related to the frequency of the TPC population.

saline-treated mice and chemotherapy-treated mice, suggesting that TPC populations do not rebound after treatment under these conditions (data not shown).

The cisplatin-etoposide combination therapy was toxic to these tumor-bearing mice when applied for longer periods, so we used cisplatin only (5 mg/kg) or control saline weekly for longer experiments (Figure 4D). Luciferase imaging confirmed that cisplatin inhibited overall tumor growth (Figure 4E). However, there was again no significant relative enrichment in CD24^{High} CD44^{Low} EpCAM^{High} populations versus non-TPCs in this assay (Figures 4F and S4C). To examine the response of single tumors to treatment, we grew isolated TKO tumors subcutaneously as allografts into NSG mice (Figure 4G). Cisplatin-treated allografts were significantly smaller than saline-treated tumors after 3 weeks of treatment, as expected (Figure 4H), but the relative frequency of CD24^{High} CD44^{Low} EpCAM^{High} cells remained the same as in the control group (Figures 4I and S4D). We recently described TKO mice carrying tumors treated weekly with cisplatin or saline until chemoresistant tumors were selected (Figure 4J) (Jahchan et al., 2013). The analysis of these chemoresistant tumors showed again no significant increase in the relative number of TPC cells versus non-TPCs (Figures 4K and S4E).

These experiments do not address how chemotherapy may affect the long-term propagation ability of CD24^{High} CD44^{Low} EpCAM^{High} cells, but they do show that these cells are neither intrinsically resistant to chemotherapeutic agents used in

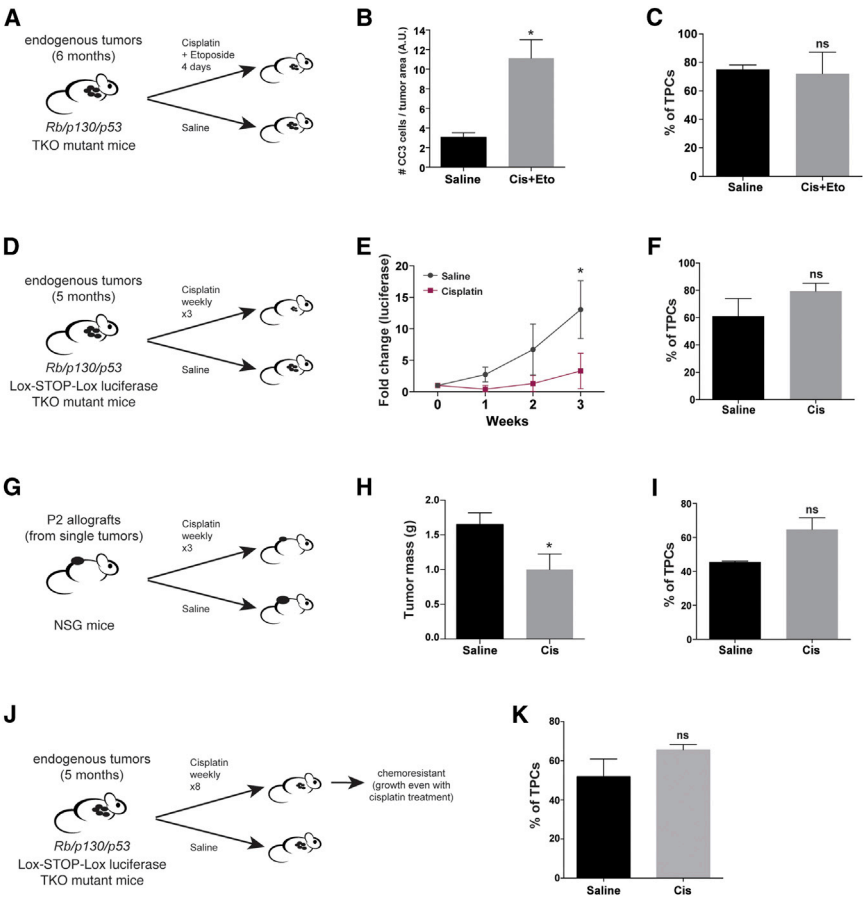

Figure 4. The Murine CD24^{High} CD44^{Low} EpCAM^{High} TPC Population Is Not Inherently Chemoresistant

(A) Strategy used for the acute treatment of *Rb/p53/p130* TKO mutant mice with saline and high doses of cisplatin (7.5 mg/kg) and etoposide (15 mg/kg) for 4 days.

(B) Analysis of CC3-positive apoptotic cells on sections from TKO tumors treated acutely with saline or cisplatin and etoposide. n = 3 mice; p = 0.0442.

(C) Relative frequency of CD24^{High} CD44^{Low} EpCAM^{High} cells from treated TKO mice. n = 3 mice; p = 0.8490.

(D) Strategy used for the treatment of *Rb/p53/p130;Rosa26$^{lox\text{-}Stop\text{-}lox\text{-}Luciferase}$* mice with saline and cisplatin (5 mg/kg) once a week for 3 weeks.

(E) Fold change of the tumor volume measured by luciferase activity in saline- and cisplatin-treated mice. n = 3 mice; p = 0.0455.

(F) Relative frequency of TPCs (CD24^{High} CD44^{Low} EpCAM^{High}) in treated mice. n = 3 mice; p = 0.2674.

(G) Strategy used for the treatment of passage P2 allografts transplanted into NSG mice from single TKO tumors; pairs were treated with saline or cisplatin (5 mg/kg) once a week for 3 weeks.

(H) Tumor mass from saline-treated allografts (n = 8 tumors) and cisplatin-treated allografts (n = 5 tumors). p = 0.0431.

(I) Relative frequency of TPCs (CD24^{High} CD44^{Low} EpCAM^{High}) in treated allografts. n = 3 mice; p = 0.1191.

(J) Strategy used for the treatment of *Rb/p53/p130;Rosa26$^{lox\text{-}Stop\text{-}lox\text{-}Luciferase}$* mice developing endogenous SCLC tumors and treated with saline or cisplatin (3 mg/kg) weekly to generate chemonaive and chemoresistant tumors (from Jahchan et al., 2013).

(K) Relative frequency of TPCs (CD24^{High} CD44^{Low} EpCAM^{High}) in treated mice. n = 3 saline-treated mice and 3 cisplatin-treated mice; p = 0.2172.

NS, not significant; error bars represent mean ± SEM; p values are from two-tailed unpaired Student's t tests. See also Figure S4.

SCLC patients nor enriched after chemoresistant tumors arise. The CDX3 and CDX4 models represent two extremes of chemotherapy response (Hodgkinson et al., 2014; C.D., unpublished data), yet in the limiting dilution studies, CDX4 tumors (the least chemosensitive) had a lower frequency of tumor-initiating cells and fewer CD24^{High} CD44^{Low} EpCAM^{High} cells compared to CDX3 tumors (most chemosensitive) (Figures 2E and 2F), uncoupling drug response from tumorigenicity. Thus, markers associated with TPCs may not be relevant biomarkers to predict relapse, and the mechanisms of chemoresistance remain poorly understood in this cancer type.

Mouse SCLC TPCs Retain Their Neuroendocrine Differentiation

To identify candidate regulators of mouse SCLC TPCs and their long-term growth properties, we compared the transcriptional profiles of CD24^{High} CD44^{Low} EpCAM^{High} cells and non-TPCs (Figure 5A). Unsupervised clustering separated the TPC and non-TPC groups (Figure S5A). Supervised clustering of genes differentially expressed at least 1.5-fold between the two populations identified 698 genes upregulated in TPCs and 1,919 upregulated in non-TPCs (Figure 5B; Table S1). Even at this low stringency for statistical cutoff, gene set enrichment analysis (GSEA) for Gene Ontology Consortium terms yielded no significantly enriched terms for TPCs, but the non-TPCs were enriched for terms related to extracellular matrix, wound remodeling, and chemokine/cytokine activity (Table S2). The analysis of oncogenic signatures revealed that the TPCs genes were enriched in a neuronal/neuroendocrine signature (CAHOY_NEURONAL) (Table S3).

Using a low-stringency approach (see Experimental Procedures), 154 genes were identified as specifically upregulated in TPCs (Table S4). A qRT-PCR analysis on an independent set of tumors confirmed the general upregulation of a few of these genes in TPCs (Figure S5B). *Ascl1* expression was increased in TPCs compared to non-TPCs (Figure S5B; Table S4). ASCL1 is a driver of neuroendocrine differentiation (Ito et al., 2000) and an oncogene in SCLC whose activity may promote the tumor-initiating capacity of SCLC cells (Augustyn et al., 2014; Jiang et al., 2009). We also found expression of the neuroendocrine marker CD56 (neural cell adhesion molecule [NCAM]) on the surface of TPCs (Figure S5C). Thus, the long-term self-renewal of mouse SCLC TPC populations is compatible with differentiated epithelial features.

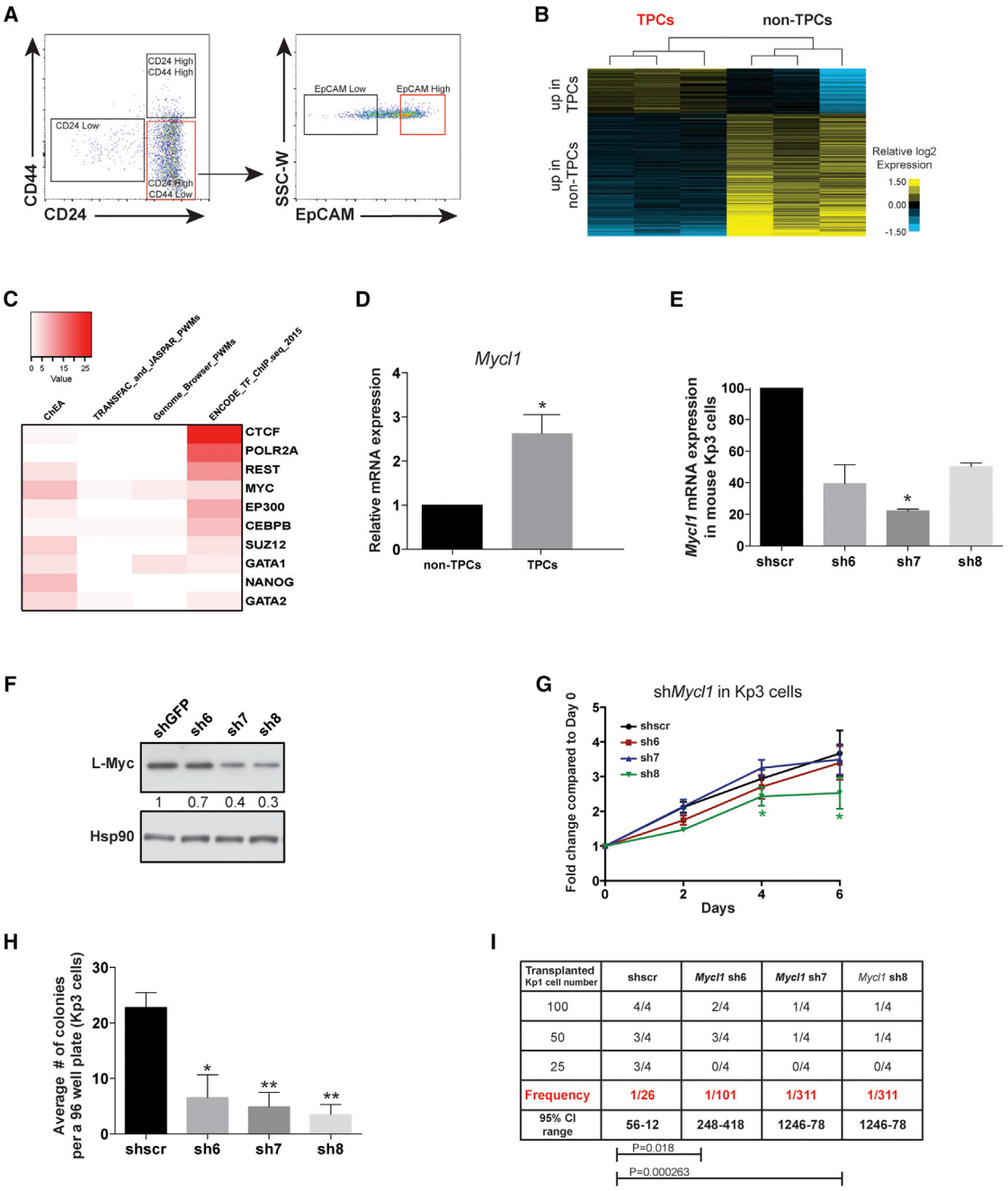

Transplanted Kp1 cell number	shscr	*Mycl1* sh6	*Mycl1* sh7	*Mycl1* sh8
100	4/4	2/4	1/4	1/4
50	3/4	3/4	1/4	1/4
25	3/4	0/4	0/4	0/4
Frequency	1/26	1/101	1/311	1/311
95% CI range	56-12	248-418	1246-78	1246-78

Figure 5. SCLC TPCs Retain Their Neuroendocrine Differentiation and Have Elevated *Mycl1* Levels

(A) Representative FACS plots to isolate TPCs (red gates, $CD24^{High}$ $CD44^{Low}$ $EpCAM^{High}$) and non-TPCs (black gates, $CD24^{Low}$, $CD24^{High}$ $CD44^{High}$, and $CD24^{High}$ $CD44^{Low}$ $EpCAM^{Low}$) populations in TKO tumors ($n \geq 3$).

(B) Heatmap of the microarray analysis comparing TPCs and non-TPCs sorted from three TKO mice. Yellow and blue indicate high and low expression, respectively. The values of the scale bar represent the median-centered log2 fold change of each gene. Hierarchical clustering was performed on genes whose expression is at least 1.5-fold different between the two groups.

(C) Top 10 overrepresented transcription factors in the TPC population (based on the total count of significantly enriched gene sets).

(D) qRT-PCR analysis of *Mycl1* mRNA levels in TPCs relative to non-TPCs (set to 1) from three TKO mice and one TKO passage P1 allograft. *Arpp0* was used as an internal control to compare the different tumors. n = 4 samples; p = 0.0323.

(E) qRT-PCR analysis of *Mycl1* mRNA levels in mouse Kp3 SCLC cells with small hairpin RNA knockdown using three hairpins (sh6, sh7, and sh8). *Arpp0* and *B-actin* were used as internal controls, and data were plotted relative to the small hairpin-scrambled vector control (shscr). n = 2 independent experiments; p = 0.0142 for sh7.

(legend continued on next page)

Elevated MYC Activity in SCLC TPCs Drives the Clonogenic Ability of SCLC Cells

We performed Enrichr analysis to identify transcriptional regulators of the 154 genes with elevated expression in TPCs. MYC was one of the top 10 overrepresented terms when counting the significantly enriched gene sets from all databases in this analysis (Figures 5C and S5D). The MYC family of transcription factors (c-MYC, L-MYC, and N-MYC) is thought to be oncogenic in SCLC (Huijbers et al., 2014; Teicher, 2014; Wistuba et al., 2001), and most human and mouse SCLC tumors express high levels of MYC factors (Figures 2B, S2A, and S2B). *Mycl1* is the most frequently amplified *Myc* family gene in mouse SCLC tumors (Calbó et al., 2005; McFadden et al., 2014; Peifer et al., 2012). Expression of *Mycl1* was specifically elevated in TPCs compared to non-TPCs (Table S1), including in an independent set of mouse tumor samples (Figure 5D). *MYCL1* levels were also higher in $CD24^{High}$ $CD44^{Low}$ $EpCAM^{High}$ cells compared to $CD24^{High}$ $CD44^{Low}$ $EpCAM^{Low}$ cells in two CDX models (Figure S5E).

To test for a possible functional role of *Mycl1* elevated levels in mouse TPCs, we knocked down *Mycl1* in murine *Rb/p53* Kp3 cells, which are nearly entirely composed of $CD24^{High}$ $CD44^{Low}$ $EpCAM^{High}$ cells (possibly by a selection process of tumorigenic cells upon passaging or simply illustrating the heterogeneity of SCLC tumors) (Figure S5F). Three independent hairpins reduced L-Myc levels 2- to 5-fold (Figures 5E and 5F) but had little to no effect on the growth of the tumor cells (Figure 5G). In contrast, the three hairpins strongly inhibited colony formation, an in vitro assay measuring the tumorigenic ability of single cells (Figure 5H). In murine *Rb/p53* mutant Kp1 cells, in which the $CD24^{High}$ $CD44^{Low}$ $EpCAM^{High}$ population represent less than half of the cells (data not shown), the sh6 hairpin knocked down *Mycl1* ~3-fold and had only modest inhibitory effects on growth, but it led to a significant decrease in the ability to form colonies (Figures S5G–S5I). $CD24^{High}$ $CD44^{Low}$ $EpCAM^{High}$ Kp1 cells formed more colonies than their $CD24^{High}$ $CD44^{Low}$ $EpCAM^{Low}$ counterparts, and *Mycl1* knockdown decreased the number of cells with TPC markers (Figures S5J and S5K). Decreased levels of *Mycl1* significantly reduced the ability of Kp1 cells to form new tumors in the flanks of NSG mice (Figure 5I). Together, these experiments show that decreasing L-Myc levels inhibits the potential for long-term growth in mouse SCLC cell lines.

JQ1 Treatment Decreases the Frequency of Mouse SCLC TPCs and Inhibits the Tumorigenic Potential of These Cells

Inhibitors of bromodomain and extra-terminal (BET) proteins can target genes highly expressed in tumors, including MYC transcription factors in SCLC and other tumors (Bauer et al., 2012; Christensen et al., 2014; Delmore et al., 2011; Filippakopoulos et al., 2010; Lovén et al., 2013; Puissant et al., 2013; Zuber et al., 2011). Treatment of Kp3 cells with escalating doses of the JQ1 inhibitor (Delmore et al., 2011) did not significantly affect the growth of these cell cultures at the lower concentrations tested (Figures 6A and S6A). In contrast, continuous JQ1 treatment strongly blocked the ability of single cells to form colonies at these lower concentrations (Figure 6B). Similar results were obtained for murine Kp1 cells (Figures S6B–S6D) and for human H69 cells (Figures S6F and S6G). The ability of various dilutions of mouse Kp1 cells to form tumors in NSG mice was significantly inhibited by JQ1 treatment at a relatively low dose (25 mg/kg daily from the day of injection, compared to 50–100 mg/kg in studies by Bolden et al., 2014; Delmore et al., 2011; and Shimamura et al., 2013) (Figure 6D). The tumors that ended up growing were smaller than control tumors, suggesting a dual effect of JQ1 on cancer re-initiation and long-term growth (Figures S6J and S6K). Pre-treatment with JQ1 for 5 days was sufficient to significantly decrease the frequency of $CD24^{High}$ $CD44^{Low}$ $EpCAM^{High}$ cells (Figure 6E), which correlated with a decreased ability to form colonies (Figure 6F) and tumors (Figure 6G). These experiments suggest that a relatively low dose of JQ1 perturbs transcriptional networks in SCLC cells that are critical for the self-renewal and the long-term growth of these tumor cells.

In all these experiments, JQ1 treatment reduced the expression of *Myc* family genes, especially *Mycl1* (Figure 6C; Figures S6E, S6H, and S6I). However, JQ1 has many more targets in cells than this gene family (Christensen et al., 2014; Lockwood et al., 2012; Tang et al., 2014). To determine whether the inhibition of the clonogenicity of SCLC cells by JQ1 was at least partly mediated by its inhibitory effect on *Myc* genes, we overexpressed mouse L-Myc from retroviral constructs whose promoter may be less affected by JQ1 than the genomic regulatory regions controlling the expression of endogenous genes. A 1.5- to 3-fold induction of L-Myc could partly rescue the effects of JQ1 treatment in a colony-formation assay in Kp3 cells (Figures 6H and 6I); a similar partial rescue was observed in Kp1 cells using a different viral vector (Figures S6L and S6M). The mechanisms by which JQ1 treatment affects the biology of SCLC TPCs are likely complex but may partly be explained by the downregulation of MYC activity.

While JQ1 treatment is clearly not equivalent to MYC inhibition, treatment with this small molecule provides a way to determine the consequences of a loss of long-term growth potential in SCLC TPCs in vivo. To test this possibility, we first repeated limited dilution transplantation assays of TPCs using mouse primary cells directly isolated from TKO tumors (Figure 7A). These

(F) Representative L-Myc immunoblotting from Kp3 cells infected with a small hairpin-control vector (shGFP) and three small hairpin-*Mycl1* vectors (sh6, sh7, and sh8). Hsp90 was used as a loading control. Quantification of the bands for L-Myc is shown below the blot.
(G) Cell growth assay (3-(4,5-dimethylthiazol-2-yl)-2,5-diphenyltetrazolium bromide [MTT]) in Kp3 cells at different days upon *Mycl1* knockdown. Fold growth is normalized to day 0. n = 4 independent biological replicas with three technical replicas each. p = 0.016 at day 4 and p = 0.0416 at day 6 for sh8; all other comparisons are not significantly different.
(H) Average of the number of colonies formed after single-cell sorting of Kp3 cells into 96-well plates. n = 3 (for sh6) and n = 4 (for sh7 and sh8) independent experiments with three technical replicas each. p = 0.0402 for sh6, p = 0.0017 for sh7, and p = 0.0079 for sh8.
(I) ELDA of shscr, sh6, sh7, and sh8 (*Mycl1* knockdown) in mouse Kp1 SCLC cells injected at different dilutions into NSG recipient mice to assess tumor formation in vivo.
Error bars represent mean ± SEM; p values are from two-tailed paired Student's t tests. See also Figure S5.

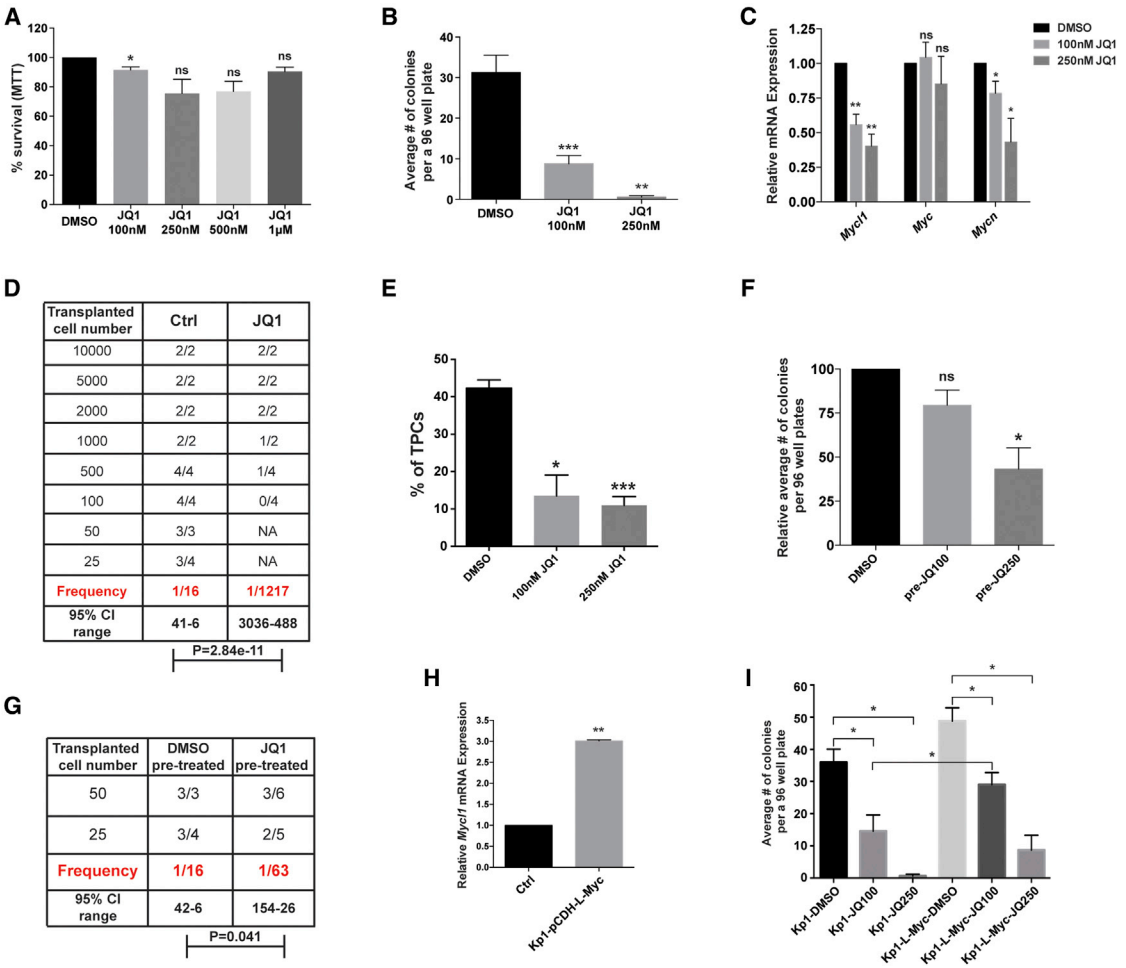

Figure 6. Lowering *Mycl1* Levels in Murine SCLC Cells with JQ1 Decreases the Frequency of TPCs and Inhibits the Tumorigenic Potential of These Cells

(A) MTT viability assay for mouse Kp1 SCLC cells after 48 hr of treatment with increasing doses of JQ1. n = 3 independent experiments; p values are for drug-treated cells versus control cells (p = 0.0222 for 100 nM JQ1).

(B) Average of the number of colonies formed after single-cell sorting of Kp1 cells into 96-well plates. n = 9 for 100 nM JQ1 and n = 7 for 250 nM JQ1; independent experiments with three technical replicas each. p = 0.0003 for 100 nM JQ1 and p = 0.0019 for 250 nM JQ1.

(C) qRT-PCR analysis of *Mycl1*, *Myc*, and *Mycn* mRNA levels in mouse Kp1 SCLC cells treated with increasing doses of JQ1 for 24 hr. *Arpp0* was used as an internal control, and the numbers were plotted relative to the DMSO-treated Kp1 cells. n = 6 independent experiments for 100 nM JQ1 and n = 4 independent experiments for 250 nM JQ1. p = 0.0010 for *Mycl1* and p = 0.0464 for *Mycn* for 100 nM JQ1; p = 0.0061 for *Mycl1* and p = 0.0450 for *Mycn* for 250 nM JQ1.

(D) ELDA of Kp1 cells injected at different dilutions into NSG recipient mice to assess the frequency of tumor formation in vivo when treated with vehicle alone (Ctrl) or with JQ1 at 25 mg/kg, starting at day 0 of transplantation and continuing for 2 weeks.

(E) Relative frequency of TPCs ($CD24^{High}$ $CD44^{Low}$ $EpCAM^{High}$) in Kp1 cells treated with DMSO or with 100 and 250 nM JQ1 for 5 days. n = 5 independent experiments. p = 0.0230 for 100 nM JQ1 and p < 0.0001 for 250 nM JQ1.

(F) Average number of colonies formed after single-cell sorting into 96 well plates of pre-treated Kp1 cells with DMSO, 100 nM JQ1 (pre-JQ100), and 250 nM JQ1 (pre-JQ250) for 5 days. n = 2 independent experiments with three technical replicas each. p = 0.0043 for pre-JQ250.

(G) ELDA of pre-treated Kp1 cells with DMSO and with 100 and 250 nM JQ1 (JQ1 pre-treated) for 5 days, injected at different dilutions into NSG recipient mice to assess the frequency of tumor formation in vivo.

(H) qRT-PCR analysis of *Mycl1* mRNA levels in Kp1 cells stably infected with the pCDH-puro-L-Myc vector relative to uninfected Kp1 cells (Ctrl) (set to 1). *Gapdh* and *Arpp0* were averaged and used as internal controls. n = 2 repeats; p = 0.0063.

(I) Number of colonies from a single-cell sort of Kp1 cells stably infected with pCDH-puro-L-Myc and control uninfected Kp1 cells in media containing DMSO, 100 nM JQ1, and 250 nM JQ1. n = 3 independent experiments. Statistical significance was determined among all groups. p = 0.046 and p = 0.013 for the effects of 100 and 250 mM JQ1, respectively; p = 0.021 for the effects of JQ1 in L-Myc-expressing cells at both 100 and 250 mM; and p = 0.0015 for the rescue effects of L-Myc on cells treated with 100 mM JQ1. The effects of L-Myc on control cells are NS.

NA, not applicable; NS, not significant; error bars represent mean ± SEM; p values are from two-tailed paired Student's t tests. See also Figure S6.

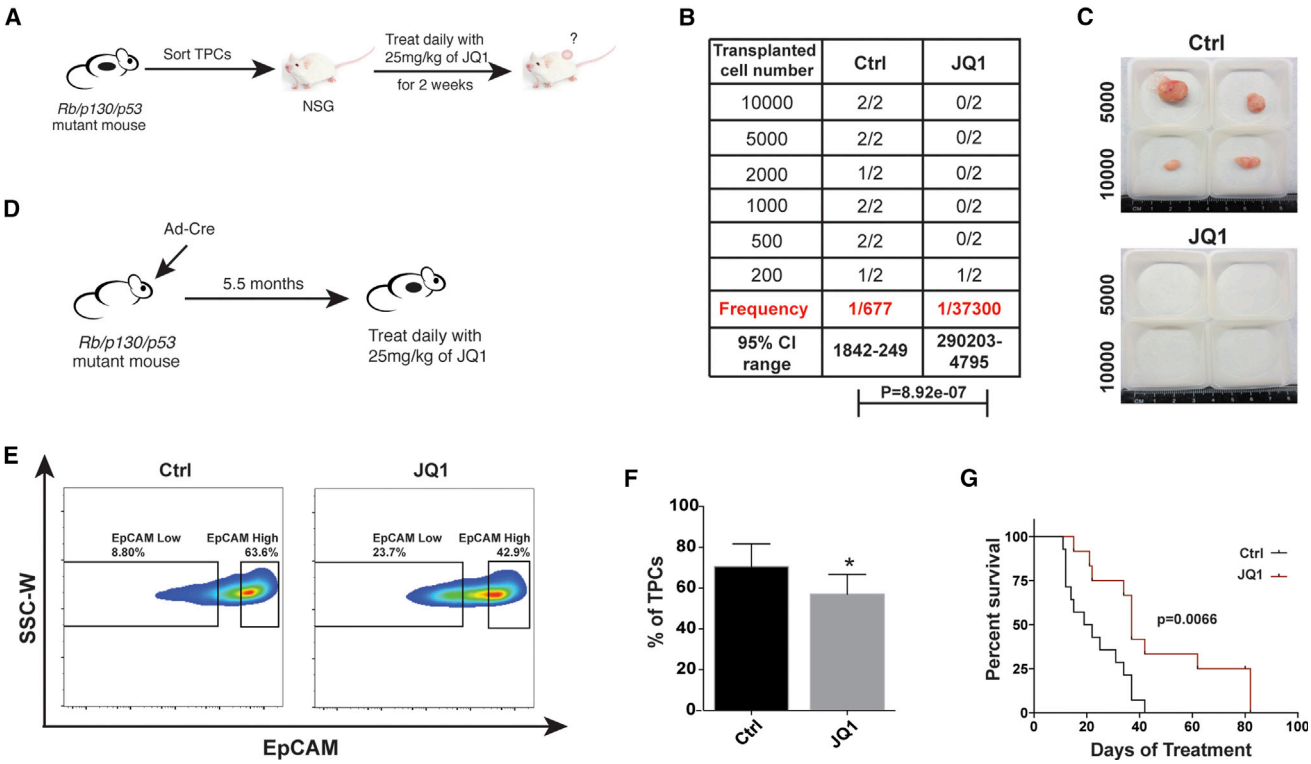

Figure 7. JQ1 Treatment Decreases the Frequency of TPCs and Inhibits Tumorigenesis in Murine Models

(A) Strategy used for sorting TPCs from TKO tumors and injecting them into recipient NSG mice treated with 25 mg/kg of JQ1 for the first 2 weeks.

(B) ELDA of the sorted TPCs in groups treated with the vehicle (control, Ctrl) or JQ1 was performed at the end of the experiment to assess the frequency of tumor formation in vivo.

(C) Representative images of the passage P1 allografts from the sorted TPCs injected in recipient NSG mice, with the number of cells indicated and treated with Ctrl or 25 mg/kg of JQ1 for the first 2 weeks.

(D) Strategy used for the treatment of TKO mice 5.5 months after Adeno-Cre instillation with 25 mg/kg of JQ1.

(E) Representative FACS plots of $CD24^{High}$ $CD44^{Low}$ $EpCAM^{High}$ and $CD24^{High}$ $CD44^{Low}$ $EpCAM^{Low}$ from tumors isolated from the Ctrl- and JQ1-treated *Rb/p53/p130* mutant mice ~1 month following treatment (n = 4).

(F) Frequency of TPCs ($CD24^{High}$ $CD44^{Low}$ $EpCAM^{High}$) in Ctrl- and JQ1-treated mice. Error bars represent mean ± SEM (n = 4 pairs); p values are from a two-tailed paired Student's t test (p = 0.0151).

(G) Survival curve generated from the *Rb/p53/p130* TKO mutant mice treated daily with intraperitoneal injections of vehicle (Ctrl) and 25 mg/kg of JQ1 starting 5.5 months after Adeno-Cre instillation (day 0 of treatment); median survival is 20.50 days for the vehicle-treated mice and 37 days for the JQ1-treated mutant mice. n = 12 vehicle-treated mice and n = 12 JQ1-treated mice; p values are from a Mantel-Cox test (p = 0.0043).

See also Figure S7.

assays showed a significant reduction in the number and the size of tumors growing in recipient mice after treatment with JQ1 compared to controls (Figures 7B and 7C), indicating that JQ1 treatment inhibits the tumor re-initiation ability of SCLC TPCs, as well as their long-term growth. Treatment of TKO; *Rosa26*$^{lox\text{-}Stop\text{-}lox\text{-}Luciferase}$ mice after 5.5 months of adenovirus-Cre recombinase (Adeno-Cre) infection with daily injections of JQ1 at 25 mg/kg (Figure 7D) decreased the frequency of the $CD24^{High}$ $CD44^{Low}$ $EpCAM^{High}$ population (Figures 7E and 7F). At that time point, treatment significantly reduced the levels of *Myc* family genes, especially *Mycl1* (Figure S7A), but did not affect the general histology of the tumors (Figure S7B). This treatment led to a significant increase in survival compared to the control group (Figure 7G), indicating that a relatively low dose of JQ1 as a single agent can have therapeutic effects in SCLC.

DISCUSSION

SCLC is the most fatal form of lung cancer. Here we found that mouse primary SCLC tumors include a significant fraction of long-term SCLC TPCs and uncovered molecular features of these TPCs that may explain the aggressive nature of these tumors and may provide new therapeutic options for SCLC patients.

Intratumoral Heterogeneity in SCLC and Significant Numbers of TPCs

Little is known about the subpopulations of tumor cells that may exist within SCLC tumors and whether these subpopulations are related to genetic or epigenetic changes (Calbó et al., 2005; Semenova et al., 2015). We found that $CD24^{High}$ $CD44^{Low}$ $EpCAM^{High}$ cells constitute around half of the cells in primary

murine SCLC tumors. The high number of TPCs is concordant with the high frequency of tumor formation from CTCs directly obtained from patients (Hodgkinson et al., 2014) and from patient-derived xenografts (PDX models) (Saunders et al., 2015). While we cannot exclude that a subpopulation of cells exists within $CD24^{High}$ $CD44^{Low}$ $EpCAM^{High}$ TPCs that may be even more potent in its transplantation ability (and possibly more quiescent and/or more chemoresistant), our current studies point to a model in which cancer stem cells comprise a large fraction of SCLC tumors and are actively cycling.

A small subset of mouse $CD44^{High}$ SCLC tumor cells expresses lower levels of neuroendocrine markers and can promote the metastasis of neuroendocrine tumor cells (Calbo et al., 2011; Kwon et al., 2015). These cells are present in the non-TPC subpopulations, but our FACS analyses indicate that other non-neuroendocrine tumor cells (defined by low or no CD56 staining) are also present in this non-TPC subgroup (data not shown). The functional interactions between TPCs and various subtypes of non-TPCs may be critical in how SCLC tumors grow, spread, and respond to treatment. However, the identities of the various subpopulations within the non-TPC group and the exact roles they may have in SCLC initiation, progression, and maintenance remain largely unknown. Better knowledge of these subpopulations may be critical to better understanding of tumor evolution and response to treatment.

Cell Surface Markers for SCLC TPCs

We found that the number of CellSearch-enumerated, $EpCAM^+$ CTCs was an independent prognostic biomarker for patient overall survival using a cutoff of 50 CTCs per 7.5 ml of blood (Hou et al., 2012). Moreover, in the 47 attempts in which we failed to generate a CDX model from a SCLC patient's blood sample, 34 of the 47 samples (72%) had an $EpCAM^+$ CTC count below this cutoff, whereas all 15 blood samples from patients for whom a CDX model was successfully derived had a $EpCAM^+$ CTC count > 50 (range 160 to >7,000). Direct comparison of CellSearch, $EpCAM^+$ CTC enumeration with a marker of independent CTC enrichment based on cell size and deformability suggests that $EpCAM^-$ SCLC CTCs also exist and may be abundant (data not shown). However, overall, these human CTC data strongly suggest that the $EpCAM^+$ CTC subpopulation has tumor-initiating capacity. These observations do not exclude that additional markers exist that would further enrich for cells with even higher transplantation ability. Thus far, our experiments show no significant differences in the transplantation ability of $CD24^{High}$ $CD44^{Low}$ $EpCAM^{High}$ cells that are $CD90^+$ compared to $CD90^-$ (frequencies of 1/320 versus 526, respectively, in these specific experiments). $CD24^{High}$ $CD44^{Low}$ $EpCAM^{High}$ c-Kit^+ and $CD24^{High}$ $CD44^{Low}$ $EpCAM^{High}$ c-Kit^- have similar calculated transplantation frequencies (1/102 versus 1/130, respectively, in these specific experiments). Other markers may be tested in the future in mouse and human models.

Rapid Emergence of Chemoresistant SCLC Is Not Explained by the TPC Model

The highly proliferative nature of TPCs in SCLC and their abundance may explain, at least partly, why these tumors are initially responsive to chemotherapy (Pietanza et al., 2015; Semenova et al., 2015). However, the mechanisms underlying the rapid relapse of chemoresistant tumors remain unexplained and do not seem to be connected to the intrinsic biology of TPCs, which indicates that the frequency of TPCs would not be a good biomarker for the growth of chemoresistant disease in patients (also seen with a PDX model in Saunders et al., 2015). The least chemosensitive CDX model (CDX4) has a lower frequency of TPCs; this suggests that specific subpopulations of non-TPCs may be more chemoresistant and might serve as protective niches for TPCs (Hartmann et al., 2005; Pardo et al., 2006). We did not observe a relative increase in $CD44^{High}$ cells (Calbo et al., 2011) after chemotherapy treatment in our mouse models (data not shown). Similarly, while CD133 expression has been correlated with chemoresistance in SCLC cell lines (Kubo et al., 2013; Sarvi et al., 2014), we did not observe an induction of this marker in mouse chemoresistant tumors (data not shown). Thus, the existence of a possible chemoresistant reservoir in SCLC remains to be ascertained.

Molecular Mechanisms Underlying the Differences between TPCs and Non-TPCs

Our gene expression studies indicate that non-TPCs are less neuroendocrine than TPCs, but we do not yet fully understand why non-TPCs are less tumorigenic than TPCs. TPCs express high levels of neuroendocrine differentiation compared to non-TPCs, including *Ascl1*, a key oncogenic factor in SCLC (Augustyn et al., 2014; Jiang et al., 2009). Accordingly, treatment with a drug-conjugated antibody against DLL3, a transcriptional target of ASCL1 (Nelson et al., 2009), was shown to inhibit the transplantation ability in human SCLC PDX models (Saunders et al., 2015). We focused on MYC based on its known oncogenic role in SCLC (Alves et al., 2014; Calbó et al., 2005; George et al., 2015; Huijbers et al., 2014; Romero et al., 2014). Emerging evidence from in vitro studies in glioblastoma (Wang et al., 2008) and pancreatic cancer (Sancho et al., 2015) suggests that elevated MYC levels are required for the self-renewal and long-term expansion of cells with features of cancer stem cells. Reducing MYC activity may be sufficient to achieve cancer inhibition without triggering the side effects that may be observed with more aggressive therapeutic interventions. However, the mechanisms by which MYC may control the self-renewal of adult stem cells and cancer stem cells are still largely unclear; in particular, whether these mechanisms overlap with the mechanism by which MYC promotes cell growth and proliferation is not known (Wilson et al., 2004). We also do not know the mechanism by which *Mycl1* transcription becomes elevated in TPCs compared to non-TPCs. In mouse neural cells, Ascl1 can directly bind to the *Mycl1* promoter region (analysis not shown of data from Webb et al., 2013) and may control its expression. It is likely that a network of transcription factors controls the fate of SCLC TPCs, including MYC and ASCL1, and this network could be affected by JQ1 treatment (Augustyn et al., 2014; Lenhart et al., 2015).

Our ability to successfully identify highly tumorigenic cancer cells in genetic and patient-derived mouse models, along with subsequent identification and targeting of transcription factors that regulate their growth, self-renewal, and survival, could

lead to more effective therapies based on the ability to eliminate TPCs rather than the bulk population of non-tumorigenic cancer cells.

EXPERIMENTAL PROCEDURES

Ethics Statement

Mice were maintained according to practices prescribed by the NIH at Stanford's Research Animal Facility accredited by the AAPLAC (protocol 13565); mice were maintained at the Stanford Research Animal Facility accredited by the Association for Assessment and Accreditation of Laboratory Animal Care. Similarly, all procedures were carried out in accordance with Home Office Regulations (UK) and the UK Coordinating Committee on Cancer Research guidelines and by approved protocols (Home Office Project license no. 40-3306 and Cancer Research UK Manchester Institute Animal Welfare and Ethical Review Advisory Board).

Human Material and Mouse Tumors

PDX and CDX models were generated from extensive stage SCLC patients after ethical approval and patient consent as previously described (Anderson et al., 2015; Hodgkinson et al., 2014). *Rb/p53/p130* TKO mice that model human SCLC have been described extensively (Gazdar et al., 2015; Jahchan et al., 2013; Park et al., 2011; Schaffer et al., 2010). For transplantation assays and analyses, SCLC tumors from TKO mice around 6–7 months of age were pooled, chopped, and then digested in 6 ml of PBS containing 120 μl of 100 mg/ml collagenase/dispase (Roche). Tumors were allowed to digest in a 37°C shaker for 45 min, followed by cooling on ice before addition of 15 μl of 1 mg/ml DNase (Sigma) for 5 min. Digested tissue was then passed through a 100 μm filter and then a 40 μm filter, and red blood cells were lysed in 1 ml of lysing solution (150 mM NH4Cl, 10 mM KHCO3, 0.1 mM EDTA), to obtain a single-cell suspension, which was counted and then stained with FACS antibodies. NSG immunocompromised mice were used for transplantation studies of allografts, and tumor cells were mixed with Matrigel (1:1) (BD Biosciences) before subcutaneous injection. For more details on the use of these models, including isolation and transplantation of single-cell suspensions, as well as drug treatments, see the Supplemental Experimental Procedures.

Cell Culture

Growth conditions for mouse and human cell lines were previously described (Jahchan et al., 2013; Park et al., 2011; Schaffer et al., 2010). For more details on the various assays used in this study, see the Supplemental Experimental Procedures.

RNA and Protein Analyses

Protocols for immunoblotting and immunostaining, as well as the analysis of RNA expression, were described previously (George et al., 2015; Jahchan et al., 2010). For more details, see the Supplemental Experimental Procedures.

Image Analysis and Statistics

Statistical significance was assayed by Student's t test with GraphPad Prism software (two-tailed unpaired and paired t test depending on the experiment). *p value < 0.05; **p value < 0.01; ***p value < 0.005; NS, not significant. Data are represented as mean ± SEM. For survival curve analysis and comparison, the Mantel-Cox test was used. For limiting dilution analyses, extreme limiting dilution analysis (ELDA) software (Hu and Smyth, 2009), which uses the frequency of tumor-positive and tumor-negative injections at each transplant dose, was used to determine the stem cell frequency or tumor formation frequency of different groups by entering the numbers of successful outgrowths and numbers of total injections for each dilution (http://bioinf.wehi.edu.au/software/elda/). Expected frequencies are reported, as well as the 95% confidence intervals (lower and upper values are indicated). The p values comparing groups were calculated by the ELDA software (see http://www.statsci.org/smyth/pubs/ELDAPreprint.pdf for more information on how p values were calculated).

ACCESSION NUMBER

The accession number for the microarray results reported in this paper is GEO: GSE72406.

SUPPLEMENTAL INFORMATION

Supplemental Information includes Supplemental Experimental Procedures, seven figures, and four tables and can be found with this article online at http://dx.doi.org/10.1016/j.celrep.2016.06.021.

AUTHOR CONTRIBUTIONS

Conceptualization, N.S.J., C.D., and J.S.; Formal Analysis, D.V., L.X., M.S.K., and J.G.; Investigation, N.S.J., J.S.L., G.S., K.Q.T., D.Y., P.K.M., S.C., T.N., W.C.A., B.B., K.M., F.T., C.J.M., and G.L.C.; Resources, F.B., C.D., S.J.D., and M.P.; Writing – Original Draft, N.S.J., J.S., and C.D.; Writing – Reviewing and Editing, N.S.J., J.S.L., B.B., K.M., G.S., K.Q.T., L.X., F.T., C.J.M., S.C., G.L.C., D.Y., D.V., M.S.K., J.G., P.K.M., T.N., W.C.A., S.J.D., F.B., M.P., C.D., and J.S. ; Visualization, N.S.J. and J.S.; Supervision, C.D., M.P., S.J.D., and J.S.; Project Administration, J.S.; Funding Acquisition, C.D., M.P., and J.S.

CONFLICTS OF INTEREST

W.C.A. and S.J.D. are shareholders in Stemcentrx, a privately held and financed company.

ACKNOWLEDGMENTS

We thank Alejandro Sweet-Cordero, Monte Winslow, and Ann Cheung for helpful comments on the study; James Bradner for providing us with JQ1; Yanyan Zheng, David Simpson, Leanne Sayles, Shaheen Sikandar, Angera Kuo, Maider Zabala, Maddalena Adorno, Kipp Weiskopf, Jens-Peter Volkmer, and Geoffrey Krampitz for suggestions and help throughout the project; and Patty Lovelace and Jennifer Ho from the FACS facility and Natalia Kosovilka from the Protein and Nucleic Acid facility for technical support. Research reported in this publication was supported by a California TRDRP post-doctoral fellowship (N.S.J. and P.K.M.), the Stanford Cancer Institute (J.S.), the Stanford Cancer Biology T32 training grant (D.Y., J.S.L., and S.C.), the Stanford Tumor Biology T32 training grant (M.S.K.), the Stanford Child Health Research Institute (J.S. and M.S.K.), A*STAR in Singapore (J.S.L.), the LUNGevity Foundation (J.S.), the German Ministry of Science and Education (BMBF) as part of the e:Med initiative (grants 01ZX1303A and 01ZX1406) (M.P.), Cancer Research UK core funding to CRUK Manchester Institute C5759/A20971 (C.D.), and the NIH (NCI R01CA201513) (J.S.). J.S. is the Harriet and Mary Zelencik Scientist in Children's Cancer and Blood Diseases.

Received: December 21, 2015
Revised: April 19, 2016
Accepted: May 31, 2016
Published: June 30, 2016

REFERENCES

Alves, R. de C.S., Meurer, R.T., and Roehe, A.V. (2014). MYC amplification is associated with poor survival in small cell lung cancer: a chromogenic in situ hybridization study. J. Cancer Res. Clin. Oncol. *140*, 2021–2025.

Anderson, W.C., Boyd, M.B., Aguilar, J., Pickell, B., Laysang, A., Pysz, M.A., Bheddah, S., Ramoth, J., Slingerland, B.C., Dylla, S.J., and Rubio, E.R. (2015). Initiation and characterization of small cell lung cancer patient-derived xenografts from ultrasound-guided transbronchial needle aspirates. PLoS ONE *10*, e0125255.

Augustyn, A., Borromeo, M., Wang, T., Fujimoto, J., Shao, C., Dospoy, P.D., Lee, V., Tan, C., Sullivan, J.P., Larsen, J.E., et al. (2014). ASCL1 is a lineage

oncogene providing therapeutic targets for high-grade neuroendocrine lung cancers. Proc. Natl. Acad. Sci. USA *111*, 14788–14793.

Bauer, D.E., Mitchell, C.M., Strait, K.M., Lathan, C.S., Stelow, E.B., Lüer, S.C., Muhammed, S., Evans, A.G., Sholl, L.M., Rosai, J., et al. (2012). Clinicopathologic features and long-term outcomes of NUT midline carcinoma. Clin. Cancer Res. *18*, 5773–5779.

Beck, B., and Blanpain, C. (2013). Unravelling cancer stem cell potential. Nat. Rev. Cancer *13*, 727–738.

Bolden, J.E., Tasdemir, N., Dow, L.E., van Es, J.H., Wilkinson, J.E., Zhao, Z., Clevers, H., and Lowe, S.W. (2014). Inducible in vivo silencing of Brd4 identifies potential toxicities of sustained BET protein inhibition. Cell Rep. *8*, 1919–1929.

Calbó, J., Meuwissen, R., van Montfort, E., van Tellingen, O., and Berns, A. (2005). Genotype-phenotype relationships in a mouse model for human small-cell lung cancer. Cold Spring Harb. Symp. Quant. Biol. *70*, 225–232.

Calbo, J., van Montfort, E., Proost, N., van Drunen, E., Beverloo, H.B., Meuwissen, R., and Berns, A. (2011). A functional role for tumor cell heterogeneity in a mouse model of small cell lung cancer. Cancer Cell *19*, 244–256.

Christensen, C.L., Kwiatkowski, N., Abraham, B.J., Carretero, J., Al-Shahrour, F., Zhang, T., Chipumuro, E., Herter-Sprie, G.S., Akbay, E.A., Altabef, A., et al. (2014). Targeting transcriptional addictions in small cell lung cancer with a covalent CDK7 inhibitor. Cancer Cell *26*, 909–922.

Chudziak, J., Burt, D.J., Mohan, S., Rothwell, D.G., Mesquita, B., Antonello, J., Dalby, S., Ayub, M., Priest, L., Carter, L., et al. (2016). Clinical evaluation of a novel microfluidic device for epitope-independent enrichment of circulating tumour cells in patients with small cell lung cancer. Analyst (Lond.) *141*, 669–678.

Clarke, M.F., Dick, J.E., Dirks, P.B., Eaves, C.J., Jamieson, C.H., Jones, D.L., Visvader, J., Weissman, I.L., and Wahl, G.M. (2006). Cancer stem cells—perspectives on current status and future directions: AACR Workshop on cancer stem cells. Cancer Res. *66*, 9339–9344.

Daniel, V.C., Marchionni, L., Hierman, J.S., Rhodes, J.T., Devereux, W.L., Rudin, C.M., Yung, R., Parmigiani, G., Dorsch, M., Peacock, C.D., and Watkins, D.N. (2009). A primary xenograft model of small-cell lung cancer reveals irreversible changes in gene expression imposed by culture in vitro. Cancer Res. *69*, 3364–3373.

Delmore, J.E., Issa, G.C., Lemieux, M.E., Rahl, P.B., Shi, J., Jacobs, H.M., Kastritis, E., Gilpatrick, T., Paranal, R.M., Qi, J., et al. (2011). BET bromodomain inhibition as a therapeutic strategy to target c-Myc. Cell *146*, 904–917.

Filippakopoulos, P., Qi, J., Picaud, S., Shen, Y., Smith, W.B., Fedorov, O., Morse, E.M., Keates, T., Hickman, T.T., Felletar, I., et al. (2010). Selective inhibition of BET bromodomains. Nature *468*, 1067–1073.

Gazdar, A.F., Savage, T.K., Johnson, J.E., Berns, A., Sage, J., Linnoila, R.I., MacPherson, D., McFadden, D.G., Farago, A., Jacks, T., et al. (2015). The comparative pathology of genetically engineered mouse models for neuroendocrine carcinomas of the lung. J. Thorac. Oncol. *10*, 553–564.

George, J., Lim, J.S., Jang, S.J., Cun, Y., Ozretić, L., Kong, G., Leenders, F., Lu, X., Fernández-Cuesta, L., Bosco, G., et al. (2015). Comprehensive genomic profiles of small cell lung cancer. Nature *524*, 47–53.

Hartmann, T.N., Burger, J.A., Glodek, A., Fujii, N., and Burger, M. (2005). CXCR4 chemokine receptor and integrin signaling co-operate in mediating adhesion and chemoresistance in small cell lung cancer (SCLC) cells. Oncogene *24*, 4462–4471.

Hodgkinson, C.L., Morrow, C.J., Li, Y., Metcalf, R.L., Rothwell, D.G., Trapani, F., Polanski, R., Burt, D.J., Simpson, K.L., Morris, K., et al. (2014). Tumorigenicity and genetic profiling of circulating tumor cells in small-cell lung cancer. Nat. Med. *20*, 897–903.

Hou, J.M., Krebs, M.G., Lancashire, L., Sloane, R., Backen, A., Swain, R.K., Priest, L.J., Greystoke, A., Zhou, C., Morris, K., et al. (2012). Clinical significance and molecular characteristics of circulating tumor cells and circulating tumor microemboli in patients with small-cell lung cancer. J. Clin. Oncol. *30*, 525–532.

Hu, Y., and Smyth, G.K. (2009). ELDA: extreme limiting dilution analysis for comparing depleted and enriched populations in stem cell and other assays. J. Immunol. Methods *347*, 70–78.

Huijbers, I.J., Bin Ali, R., Pritchard, C., Cozijnsen, M., Kwon, M.C., Proost, N., Song, J.Y., de Vries, H., Badhai, J., Sutherland, K., et al. (2014). Rapid target gene validation in complex cancer mouse models using re-derived embryonic stem cells. EMBO Mol. Med. *6*, 212–225.

Ito, T., Udaka, N., Yazawa, T., Okudela, K., Hayashi, H., Sudo, T., Guillemot, F., Kageyama, R., and Kitamura, H. (2000). Basic helix-loop-helix transcription factors regulate the neuroendocrine differentiation of fetal mouse pulmonary epithelium. Development *127*, 3913–3921.

Jahchan, N.S., You, Y.H., Muller, W.J., and Luo, K. (2010). Transforming growth factor-beta regulator SnoN modulates mammary gland branching morphogenesis, postlactational involution, and mammary tumorigenesis. Cancer Res. *70*, 4204–4213.

Jahchan, N.S., Dudley, J.T., Mazur, P.K., Flores, N., Yang, D., Palmerton, A., Zmoos, A.F., Vaka, D., Tran, K.Q., Zhou, M., et al. (2013). A drug repositioning approach identifies tricyclic antidepressants as inhibitors of small cell lung cancer and other neuroendocrine tumors. Cancer Discov. *3*, 1364–1377.

Jiang, T., Collins, B.J., Jin, N., Watkins, D.N., Brock, M.V., Matsui, W., Nelkin, B.D., and Ball, D.W. (2009). Achaete-scute complex homologue 1 regulates tumor-initiating capacity in human small cell lung cancer. Cancer Res. *69*, 845–854.

Krebs, M.G., Metcalf, R.L., Carter, L., Brady, G., Blackhall, F.H., and Dive, C. (2014). Molecular analysis of circulating tumour cells-biology and biomarkers. Nat. Rev. Clin. Oncol. *11*, 129–144.

Kubo, T., Takigawa, N., Osawa, M., Harada, D., Ninomiya, T., Ochi, N., Ichihara, E., Yamane, H., Tanimoto, M., and Kiura, K. (2013). Subpopulation of small-cell lung cancer cells expressing CD133 and CD87 show resistance to chemotherapy. Cancer Sci. *104*, 78–84.

Kwon, M.C., Proost, N., Song, J.Y., Sutherland, K.D., Zevenhoven, J., and Berns, A. (2015). Paracrine signaling between tumor subclones of mouse SCLC: a critical role of ETS transcription factor Pea3 in facilitating metastasis. Genes Dev. *29*, 1587–1592.

Lenhart, R., Kirov, S., Desilva, H., Cao, J., Lei, M., Johnston, K., Peterson, R., Schweizer, L., Purandare, A., Ross-Macdonald, P., et al. (2015). Sensitivity of small cell lung cancer to BET inhibition is mediated by regulation of ASCL1 gene expression. Mol. Cancer Ther. *14*, 2167–2174.

Leong, T.L., Marini, K.D., Rossello, F.J., Jayasekara, S.N., Russell, P.A., Prodanovic, Z., Kumar, B., Ganju, V., Alamgeer, M., Irving, L.B., et al. (2014). Genomic characterisation of small cell lung cancer patient-derived xenografts generated from endobronchial ultrasound-guided transbronchial needle aspiration specimens. PLoS ONE *9*, e106862.

Lockwood, W.W., Zejnullahu, K., Bradner, J.E., and Varmus, H. (2012). Sensitivity of human lung adenocarcinoma cell lines to targeted inhibition of BET epigenetic signaling proteins. Proc. Natl. Acad. Sci. USA *109*, 19408–19413.

Lovén, J., Hoke, H.A., Lin, C.Y., Lau, A., Orlando, D.A., Vakoc, C.R., Bradner, J.E., Lee, T.I., and Young, R.A. (2013). Selective inhibition of tumor oncogenes by disruption of super-enhancers. Cell *153*, 320–334.

Magee, J.A., Piskounova, E., and Morrison, S.J. (2012). Cancer stem cells: impact, heterogeneity, and uncertainty. Cancer Cell *21*, 283–296.

McFadden, D.G., Papagiannakopoulos, T., Taylor-Weiner, A., Stewart, C., Carter, S.L., Cibulskis, K., Bhutkar, A., McKenna, A., Dooley, A., Vernon, A., et al. (2014). Genetic and clonal dissection of murine small cell lung carcinoma progression by genome sequencing. Cell *156*, 1298–1311.

Meacham, C.E., and Morrison, S.J. (2013). Tumour heterogeneity and cancer cell plasticity. Nature *501*, 328–337.

Meuwissen, R., Linn, S.C., Linnoila, R.I., Zevenhoven, J., Mooi, W.J., and Berns, A. (2003). Induction of small cell lung cancer by somatic inactivation of both Trp53 and Rb1 in a conditional mouse model. Cancer Cell *4*, 181–189.

Micke, P., Basrai, M., Faldum, A., Bittinger, F., Rönnstrand, L., Blaukat, A., Beeh, K.M., Oesch, F., Fischer, B., Buhl, R., and Hengstler, J.G. (2003).

Characterization of c-kit expression in small cell lung cancer: prognostic and therapeutic implications. Clin. Cancer Res. *9*, 188–194.

Nelson, B.R., Hartman, B.H., Ray, C.A., Hayashi, T., Bermingham-McDonogh, O., and Reh, T.A. (2009). Acheate-scute like 1 (Ascl1) is required for normal delta-like (Dll) gene expression and notch signaling during retinal development. Dev. Dyn. *238*, 2163–2178.

Pardo, O.E., Wellbrock, C., Khanzada, U.K., Aubert, M., Arozarena, I., Davidson, S., Bowen, F., Parker, P.J., Filonenko, V.V., Gout, I.T., et al. (2006). FGF-2 protects small cell lung cancer cells from apoptosis through a complex involving PKCepsilon, B-Raf and S6K2. EMBO J. *25*, 3078–3088.

Park, K.S., Martelotto, L.G., Peifer, M., Sos, M.L., Karnezis, A.N., Mahjoub, M.R., Bernard, K., Conklin, J.F., Szczepny, A., Yuan, J., et al. (2011). A crucial requirement for Hedgehog signaling in small cell lung cancer. Nat. Med. *17*, 1504–1508.

Peifer, M., Fernández-Cuesta, L., Sos, M.L., George, J., Seidel, D., Kasper, L.H., Plenker, D., Leenders, F., Sun, R., Zander, T., et al. (2012). Integrative genome analyses identify key somatic driver mutations of small-cell lung cancer. Nat. Genet. *44*, 1104–1110.

Pietanza, M.C., Byers, L.A., Minna, J.D., and Rudin, C.M. (2015). Small cell lung cancer: will recent progress lead to improved outcomes? Clin. Cancer Res. *21*, 2244–2255.

Puissant, A., Frumm, S.M., Alexe, G., Bassil, C.F., Qi, J., Chanthery, Y.H., Nekritz, E.A., Zeid, R., Gustafson, W.C., Greninger, P., et al. (2013). Targeting MYCN in neuroblastoma by BET bromodomain inhibition. Cancer Discov. *3*, 308–323.

Quintana, E., Shackleton, M., Foster, H.R., Fullen, D.R., Sabel, M.S., Johnson, T.M., and Morrison, S.J. (2010). Phenotypic heterogeneity among tumorigenic melanoma cells from patients that is reversible and not hierarchically organized. Cancer Cell *18*, 510–523.

Romero, O.A., Torres-Diz, M., Pros, E., Savola, S., Gomez, A., Moran, S., Saez, C., Iwakawa, R., Villanueva, A., Montuenga, L.M., et al. (2014). MAX inactivation in small cell lung cancer disrupts MYC-SWI/SNF programs and is synthetic lethal with BRG1. Cancer Discov. *4*, 292–303.

Rygaard, K., Nakamura, T., and Spang-Thomsen, M. (1993). Expression of the proto-oncogenes c-met and c-kit and their ligands, hepatocyte growth factor/scatter factor and stem cell factor, in SCLC cell lines and xenografts. Br. J. Cancer *67*, 37–46.

Salcido, C.D., Larochelle, A., Taylor, B.J., Dunbar, C.E., and Varticovski, L. (2010). Molecular characterisation of side population cells with cancer stem cell-like characteristics in small-cell lung cancer. Br. J. Cancer *102*, 1636–1644.

Sancho, P., Burgos-Ramos, E., Tavera, A., Bou Kheir, T., Jagust, P., Schoenhals, M., Barneda, D., Sellers, K., Campos-Olivas, R., Graña, O., et al. (2015). MYC/PGC-1α balance determines the metabolic phenotype and plasticity of pancreatic cancer stem cells. Cell Metab. *22*, 590–605.

Sarvi, S., Mackinnon, A.C., Avlonitis, N., Bradley, M., Rintoul, R.C., Rassl, D.M., Wang, W., Forbes, S.J., Gregory, C.D., and Sethi, T. (2014). CD133+ cancer stem-like cells in small cell lung cancer are highly tumorigenic and chemoresistant but sensitive to a novel neuropeptide antagonist. Cancer Res. *74*, 1554–1565.

Saunders, L.R., Bankovich, A.J., Anderson, W.C., Aujay, M.A., Bheddah, S., Black, K., Desai, R., Escarpe, P.A., Hampl, J., Laysang, A., et al. (2015). A DLL3-targeted antibody-drug conjugate eradicates high-grade pulmonary neuroendocrine tumor-initiating cells in vivo. Sci. Transl. Med. *7*, 302ra136.

Schaffer, B.E., Park, K.S., Yiu, G., Conklin, J.F., Lin, C., Burkhart, D.L., Karnezis, A.N., Sweet-Cordero, E.A., and Sage, J. (2010). Loss of p130 accelerates tumor development in a mouse model for human small-cell lung carcinoma. Cancer Res. *70*, 3877–3883.

Semenova, E.A., Nagel, R., and Berns, A. (2015). Origins, genetic landscape, and emerging therapies of small cell lung cancer. Genes Dev. *29*, 1447–1462.

Shafee, N., Smith, C.R., Wei, S., Kim, Y., Mills, G.B., Hortobagyi, G.N., Stanbridge, E.J., and Lee, E.Y. (2008). Cancer stem cells contribute to cisplatin resistance in Brca1/p53-mediated mouse mammary tumors. Cancer Res. *68*, 3243–3250.

Shimamura, T., Chen, Z., Soucheray, M., Carretero, J., Kikuchi, E., Tchaicha, J.H., Gao, Y., Cheng, K.A., Cohoon, T.J., Qi, J., et al. (2013). Efficacy of BET bromodomain inhibition in Kras-mutant non-small cell lung cancer. Clin. Cancer Res. *19*, 6183–6192.

Tang, Y., Gholamin, S., Schubert, S., Willardson, M.I., Lee, A., Bandopadhayay, P., Bergthold, G., Masoud, S., Nguyen, B., Vue, N., et al. (2014). Epigenetic targeting of Hedgehog pathway transcriptional output through BET bromodomain inhibition. Nat. Med. *20*, 732–740.

Teicher, B.A. (2014). Targets in small cell lung cancer. Biochem. Pharmacol. *87*, 211–219.

Vaillant, F., Asselin-Labat, M.L., Shackleton, M., Forrest, N.C., Lindeman, G.J., and Visvader, J.E. (2008). The mammary progenitor marker CD61/beta3 integrin identifies cancer stem cells in mouse models of mammary tumorigenesis. Cancer Res. *68*, 7711–7717.

Visvader, J.E., and Lindeman, G.J. (2012). Cancer stem cells: current status and evolving complexities. Cell Stem Cell *10*, 717–728.

Wang, J., Wang, H., Li, Z., Wu, Q., Lathia, J.D., McLendon, R.E., Hjelmeland, A.B., and Rich, J.N. (2008). c-Myc is required for maintenance of glioma cancer stem cells. PLoS ONE *3*, e3769.

Wang, P., Gao, Q., Suo, Z., Munthe, E., Solberg, S., Ma, L., Wang, M., Westerdaal, N.A., Kvalheim, G., and Gaudernack, G. (2013). Identification and characterization of cells with cancer stem cell properties in human primary lung cancer cell lines. PLoS ONE *8*, e57020.

Webb, A.E., Pollina, E.A., Vierbuchen, T., Urbán, N., Ucar, D., Leeman, D.S., Martynoga, B., Sewak, M., Rando, T.A., Guillemot, F., et al. (2013). FOXO3 shares common targets with ASCL1 genome-wide and inhibits ASCL1-dependent neurogenesis. Cell Rep. *4*, 477–491.

Wilson, A., Murphy, M.J., Oskarsson, T., Kaloulis, K., Bettess, M.D., Oser, G.M., Pasche, A.C., Knabenhans, C., Macdonald, H.R., and Trumpp, A. (2004). c-Myc controls the balance between hematopoietic stem cell self-renewal and differentiation. Genes Dev. *18*, 2747–2763.

Wistuba, I.I., and Gazdar, A.F. (2006). Lung cancer preneoplasia. Annu. Rev. Pathol. *1*, 331–348.

Wistuba, I.I., Gazdar, A.F., and Minna, J.D. (2001). Molecular genetics of small cell lung carcinoma. Semin. Oncol. *28* (*2, Suppl 4*), 3–13.

Zheng, Y., de la Cruz, C.C., Sayles, L.C., Alleyne-Chin, C., Vaka, D., Knaak, T.D., Bigos, M., Xu, Y., Hoang, C.D., Shrager, J.B., et al. (2013). A rare population of CD24(+)ITGB4(+)Notch(hi) cells drives tumor propagation in NSCLC and requires Notch3 for self-renewal. Cancer Cell *24*, 59–74.

Zuber, J., Shi, J., Wang, E., Rappaport, A.R., Herrmann, H., Sison, E.A., Magoon, D., Qi, J., Blatt, K., Wunderlich, M., et al. (2011). RNAi screen identifies Brd4 as a therapeutic target in acute myeloid leukaemia. Nature *478*, 524–528.